A Turnkey Data Logger Program for Field-Scale Energy Flux Density Measurements Using Eddy Covariance and Surface Renewal

*Thomas M. Shapland [1], Andrew J. McElrone [1,2], Khaw Tha Paw U [3], Richard L. Snyder [3]**

Abstract: *Micrometeorological methods and ecosystem-scale energy and mass flux density measurements have become increasingly important in soil, agricultural, and environmental sciences. For many scientists without formal training in atmospheric science, these techniques are relatively inaccessible. Eddy covariance, surface renewal, and other flux measurement methods require an understanding of boundary layer meteorology and extensive training in instrumentation and multiple data processing programs. In this paper, we present an open-source turnkey data logger program that performs flux data acquisition and post-processing, returning to the user a simple data table with the corrected energy balance fluxes and quality control parameters. The underlying theory of the flux measurements is briefly discussed and the program design and execution are described line by line. Data were collected over a wheat canopy and the program results were tested against other flux processing software, including EdiRe and R. The energy balance fluxes appear reasonable for the fair weather conditions found during data collection period. The daily cumulative evapotranspiration values from the flux tower and logger program show strong agreement with measurements from a precision weighing lysimeter. The logger program can be accessed at sites.google.com/site/tmshapland.*
Keywords: *atmospheric surface-layer fluxes, energy balance, evapotranspiration, latent heat flux density, lysimetry, micrometeorology.*

Riassunto: *I metodi micro-meteorologici e le misure dei flussi di massa e di energia alla scala di ecosistema hanno recentemente acquisito importanza nelle scienze agrarie, del suolo e dell'ambiente. Queste tecniche sono relativamente inaccessibili ai molti ricercatori che non abbiano una preparazione tecnica in meteorologia. Eddy covariance, surface renewal e altri metodi per la misura dei flussi richiedono familiarita' con i fondamenti della meteorologia dello strato di confine atmosferico ed una profonda conoscenza della strumentazione e dei programma di analisi dei dati. In questo articolo presentiamo un programma open source pronto all'uso per l'acquisizione e l'analisi di dati, che fornisce come risultato una semplice tabella con i flussi di energia corretti ed i parametri di controllo dei dati. La teoria alla base delle misurazioni è brevemente discussa e la struttura e l'esecuzione del programma sono descritte linea per linea. I dati sono stati acquisiti su una coltura di frumento ed i risultati del programma sono stati validati in comparazione con altri programmi di analisi di dati di flusso, fra cui EdiRe e R. I flussi del bilancio energetico appaiono ragionevoli per le condizioni di bel tempo del periodo di raccolta dati. I valori cumulati giornalieri di evapotraspirazione, provenienti dalla torre di misura dei flussi e dal datalogger, mostrano un'ottima corripondenza con i dati misurati da un lisimetro a pesata di precisione. Il programma per datalogger può essere scaricato dal sito: sites.google.com/site/tmshapland.*
Parole chiave: *flussi atmosferici nello strato di confine, bilancio energetico, evapotraspirazione, flusso di calore latente, micrometeorologia, sistemi di misura online.*

1. INTRODUCTION

The measurement of ecosystem-scale energy and mass flux densities is important in the study of agrometeorology, especially as climate change, environmental policy, and growing urban demands limit agricultural water resources (e.g., California Department of Water Resources, 2005). Agrometeorologists measure evapotranspiration (*ET*) to evaluate experimental treatments for improving crop water use efficiency (e.g., Moratiel and Martinez-Cob, 2011), to provide growers with crop coefficient information (Doorenbos and Pruitt, 1977), and to parameterize regional water allocation strategies (Snyder *et al.*, 2005). Evapotranspiration measurements also have the potential to empower growers with site-specific crop water demand and irrigation management information. Eddy covariance (Swinbank, 1951) and surface renewal (Paw U *et al.*, 1995) are two methods for measuring turbulent fluxes such as sensible heat flux density (*H*).

* Corresponding author.
R.L. Snyder e-mail: rlsnyder@ucdavis.edu
[1] Department of Viticulture & Enology, University of California, Davis, CA, U.S.A.
[2] United States Department of Agriculture-Agricultural Research Service, Crops Pathology and Genetics Research Unit, Davis, CA, U.S.A.
[3] Atmospheric Science, University of California, Davis, CA, U.S.A.
Received 7 August 2012, accepted 29 November 2012.

When H measurements are taken in conjunction with net radiation (Rn) and ground heat flux density (G) measurements or estimates, latent heat flux density (λE) can be calculated from the energy balance residual, providing an inexpensive approach to estimate ET.

The successful deployment of an eddy covariance flux tower for ET measurements can be a daunting challenge, especially for many agricultural researchers without formal training in atmospheric science. Eddy covariance and surface renewal measurements require sophisticated technical skills in both programming data loggers to execute tasks with complex instrumentation and writing computer programs to post-process the raw turbulence data into meaningful fluxes. Furthermore, because high-frequency measurements are needed for both eddy covariance and surface renewal, agrometeorologists face the additional challenge of managing vast amounts of data. Even for experienced agrometeorologists with theoretical and practical expertise in ecosystem-scale flux measurements, data management and post-processing are tedious and time-consuming endeavors.

We have developed a turnkey data logger program for ET measurements that streamlines the data collection and post-processing procedures, facilitating access to micrometeorology for neophytes and adding convenience for experienced flux scientists. The program collects and stores raw data from the Rn, G, and H sensors. The raw data are processed in the logger program, appropriate corrections are applied, and the corrected fluxes, including λE from the energy balance residual, are output on a simple and convenient data table. In this paper we summarize the theoretical basis of the flux calculations, describe the design and execution of the program, and validate the program against other flux processing software using data collected over a wheat canopy. The logger program results agree well with lysimeter measurements and with the expected course of diurnal energy balance fluxes during fair weather conditions.

2. EXPERIMENTAL DATA, INSTRUMENTATION, AND ANALYSIS

The program was installed in a CR1000 data logger (Campbell Scientific Inc., Logan, UT, U.S.A.) and tested over a wheat canopy from February 14 2012 to June 12 2012 at the Campbell Tract at the University of California, Davis (38°32'N, 121°46'W). The data presented in this paper are from five contiguous days, April 19 2012 to April 23 2012 (Day of year 111 to 115), when the meteorological conditions were typical for the region and season, i.e., clear and sunny, allowing for a detailed comparison of the expected energy balance fluxes and the output of the logger program. The wheat canopy height was 0.9 m and fetch was 100 m in the prevailing wind direction (south). The three-dimensional wind velocities and sonic temperature were sampled at 10 Hz with a sonic anemometer (81000RE, R.M. Young Company, Traverse City, MO, U.S.A) installed at 1.6 m above the ground (Tab. 1). Note that the sonic anemometer requires reconfiguration from the factory settings prior to field deployment to output the desired signals (For more information, see *RM Young Model 81000RE Reconfiguration Instructions.pdf* available at sites.google.com/site/ tmshapland). The air temperature was also sampled at 10 Hz with a 76 µm diameter fine wire thermocouple (FW3, Campbell Scientific Inc., Logan, UT, U.S.A.) located at 1.35 m above the ground, and net radiation measured with a net radiometer (NR-Lite, Kipp & Zonen B.V., Delft, The Netherlands) at 1.80 m above the ground. Two soil heat flux plates (HFT-3.1, REBS Inc., Seattle, WA, U.S.A.) were buried 0.05 m below the soil surface, and a soil thermocouple (TCAV, Campbell Scientific Inc., Logan, UT, U.S.A.) was installed to span the volume of soil above the heat flux plate and provide temperature change to estimate the surface ground heat flux associated with heat storage above the plates.

Evapotranspiration data were also collected from a 6.1 m diameter weighing lysimeter (Pruitt and Angus, 1960). The flux tower was located approximately 15 m to the west of the lysimeter. The plants inside the lysimeter were slightly less densely spaced and about 10 cm shorter than plants in the surrounding field.

The energy balance terms calculated by the logger program were tested against EdiRe flux processing software (Mauder *et al.*, 2008) and functions written in the R statistical environment (R Development Core Team, 2012).The comparison analysis among software programs and graphics generation were performed in R.

3. FLUX MEASUREMENT THEORY

3.1. Net radiation

Net radiation is the total incoming radiation impinging on the surface minus the total outgoing radiation. Like many net radiometers, the sensor used in this study absorbs short and long waveband radiation on both sides of the sensor. The voltage output depends on the difference between the radiation received from the upper and lower surface of the sensor, and the voltage reading is converted from volts to energy flux density using a calibration factor determined by the manufacturer.

3.2. Ground heat flux density

Ground heat flux density is energy conducted into or out of the ground. It can be measured using a ground

Sensor	Model	Manufacturer	Sensor wire color or port	Data logger channel or port
Air thermocouple	FW3	Campbell Scientific Inc.	Purple	1H
			Red	1L
			Clear	Signal ground
Net radiometer	NR-Lite	Kipp & Zonen B.V.	White	2H
			Green	2L
			Shield (bare)	Signal ground
			Jumper wire	2L to Signal ground
Ground heat flux plate	HFT-3.1	REBS Inc.	Black	3H
			Red	3L
			Shield (bare)	Signal ground
Ground heat flux plate	HFT-3.1	REBS Inc.	Black	4H
			Red	4L
			Shield (bare)	Signal ground
Soil thermocouple	TCAV	Campbell Scientific Inc.	Purple	5H
			Red	5L
			Shield (bare)	Signal ground
Sonic anemometer	81000RE	R.M. Young	RX	C7
		Company	TX	C8
			Serial reference	G
			+PWR	12V
			PWR reference	G
			Earth ground	G

Tab. 1 - Instrumentation and wiring diagram.
Tab. 1 - Strumentazione e diagramma di connessione dei cavi.

heat flux plate and soil temperature sensors. The thermopile inside the ground heat flux plate measures the temperature gradient across a material with known thermal properties to arrive at the energy flux density. Each plate is calibrated by the manufacturer. Because ground heat flux plates cannot be placed directly on top of the soil without intercepting solar radiation, they must be buried below the soil surface. The energy flux density at the depth of the ground heat flux plates is not the same at the energy flux density at the surface because some energy is stored in the soil layer above the plate, so a set of soil thermocouples wired in parallel are installed in the layer above the plates. The following continuity equation is used with the heat flux plate output and the change in heat storage within the soil layer above the plates to estimate the ground heat flux G at the surface:

$$G = G' + \Delta S \tag{1}$$

where G' is the ground heat flux density at the plates and ΔS is the change in heat storage per unit area in the soil layer above the heat flux plates. The latter term is expressed as

$$\Delta S = C_v \left(\frac{T_f - T_i}{t_f - t_i} \right) d_g \tag{2}$$

where T_f is the final temperature (K) at time t_f and T_i is the initial temperature (K) at time t_i, d_g is the depth (m) from the soil surface to the heat flux plates, and C_v is the volumetric heat capacity (J m^{-3} K^{-1}). Soil volumetric heat capacity can be estimated according to de Vries (1963) and Jensen, Burman, and Allen (1990).

$$C_v = \left(1.93 V_m + 2.51 V_o + 4.19\theta\right) 10^6 \tag{3}$$

where (V_m) is the volume fractions of minerals, (V_o) is the volume fraction of organic matter, and (Θ) is the volumetric water content. Since V_o is typically small and the soil bulk density (P_b) is related to V_m, one can also estimate C_v using the equation:

$$C_v = \left(0.837 \rho_b + 4.19\theta\right) 10^6 \tag{4}$$

The factor 10^6 converts the soil and water densities

from Mg m^{-3} to g m^{-3}. Multiplying the densities by the apparent specific heats for soil and water, 0.837 (J g^{-1} K^{-1}) and 4.19 (J g^{-1} K^{-1}), respectively, gives C_v in J m^{-3} K^{-1}. In the logger program, the soil bulk density is assigned a default value of 1.3 Mg m^{-3} and the volumetric water content is assigned a default value of 0.2, although the logger program can be modified to include other default values or to make measurements with volumetric water content sensors. The soil heat flux density is usually less than 15% of *Rn*, so small errors in the soil heat flux storage term in the thin soil layer above the plates, caused by differences between the default soil parameters and the actual soil characteristics, should not create large errors in the λE calculation.

3.3. Sensible heat flux density

Sensible heat flux density is the energy flux density from the surface to the air or vice-versa. The logger program calculates *H* using both the eddy covariance and surface renewal techniques.

3.3.1. Eddy covariance

Eddy covariance measures the turbulent fluctuations in vertical wind speed and the air temperature to arrive at *H* (Swinbank, 1951) with the following equation:

$$H = \rho C_p \left(\overline{w'T_s'}\right) \tag{5}$$

where ρ is the air density (g m^{-3}), *Cp* is the specific heat per unit mass of air at constant pressure (J g^{-1} K^{-1}),w, is the vertical wind velocity (m s^{-1})^{Ts}, is the sonic temperature (K), the prime signifies the instantaneous departure from the mean and the overbar denotes a time-averaged interval.

To eliminate a major source of error in eddy covariance measurements, a two-dimensional coordinate rotation correction is applied in the logger to force the mean cross and vertical wind velocities to zero (Tanner and Thurtell, 1969). The rotation angles are calculated as follows:

$$\sin\theta = \frac{\overline{w}}{\sqrt{\overline{u}^2 + \overline{v}^2 + \overline{w}^2}} \tag{6a}$$

$$\cos\theta = \frac{\sqrt{\overline{u}^2 + \overline{v}^2}}{\sqrt{\overline{u}^2 + \overline{v}^2 + \overline{w}^2}} \tag{6b}$$

$$\sin\eta = \frac{\overline{v}}{\sqrt{\overline{u}^2 + \overline{v}^2}} \tag{6c}$$

$$\cos\eta = \frac{\overline{u}}{\sqrt{\overline{u}^2 + \overline{v}^2}} \tag{6d}$$

The trigonometric functions are used to calculate the tilt-corrected sonic temperature flux:

$$\overline{w'T_S'} = \overline{w'T_S'}_{raw} \cos\theta - \overline{u'T'}_{S\,raw} \sin\theta\cos\eta - \overline{v'T'}_{S\,raw} \sin\theta\sin\eta \tag{7}$$

and the tilt-corrected momentum flux density normalized by air density:

$$\overline{u'w'} = \overline{u'w'}_{raw} \cos\eta\left(\cos^2\theta - \sin^2\theta\right) + \overline{v'w'}_{raw} \sin\eta\left(\cos^2\theta - \sin^2\theta\right) + \overline{(w')^2}_{raw} \sin\theta\cos\theta - \overline{(u')^2}_{raw} \sin\theta\cos\theta\cos^2\eta - \overline{(v')^2_{raw}} \sin\theta\cos\theta\sin^2\eta - 2\overline{u'v'}_{raw} \sin\theta\cos\theta\sin\eta\cos\eta \tag{8}$$

3.3.2. Surface renewal

Surface renewal is based on analyzing the energy budget of air parcels, or coherent structures, that reside ephemerally within the crop canopy during the turbulent exchange process (Paw U *et al.*, 1995). The air parcels are manifested as ramp-like shapes in turbulent temperature time series data, and the amplitude and period of the ramps are used to calculate the flux density.

$$H = \alpha z \rho C_p \frac{a}{\tau} \tag{9}$$

where α is the alpha calibration factor, z is the measurement height (m), a is the ramp amplitude (K), and τ is the ramp period (s). Surface renewal flux density measurements are calibrated against an independent flux measurement technique, such as eddy covariance. The alpha calibration is obtained as the slope of the least squares linear regression forced through the origin, and its value depends on sensor height, canopy height, canopy architecture, atmospheric stability, turbulent characteristics, and sensor dynamic response characteristics (Paw U *et al.*, 1995; Paw U *et al.*, 2005). In the logger program, the alpha calibration is assumed to be unity unless the user changes the default value. By setting alpha to a default value of one, the surface renewal values output by the logger program have not been calibrated. Once the calibration has been determined, the user can change the default value of the alpha calibration to the actual alpha calibration.

The Van Atta (1977) procedure is used to resolve the ramp amplitude and ramp period from the air temperature data for the surface renewal calculation (Paw U *et al.*, 1995; Spano *et al.*, 1997). In the first step of the procedure, the structure function is calculated from the high frequency air temperature data.

$$\overline{S^n(r)} = \frac{1}{m-j}\sum_{k=1}^{m-j}\left[\left(T_k - T_{k-j}\right)^n\right] \tag{10}$$

where $\overline{S^n(r)}$ is the nth-order structure function, m is the number of points in the time series, j is the sample lag between points, TK is the element in the scalar time series. The time lag (r) is calculated as the sample lag divided by the sampling frequency ($r = j / f$). The structure function values constitute the coefficients in the following cubic polynomial:

$$0 = a^3 + pa + q \tag{11a}$$

where

$$p = \left[10\overline{S^2(r)} - \frac{\overline{s^5(r)}}{\overline{s^3(r)}}\right] \tag{11b}$$

and

$$q = 10S^3(r) \tag{11c}$$

Equation (11a) is solved in the logger program using an analytical solution method to obtain the ramp amplitude. The ramp period is calculated from the ramp amplitude, the structure function time lag, and the third-order structure function, as follows:

$$d + s = -\frac{a^3 r}{S^3 r} \tag{12}$$

Although it is not shown here for the sake of brevity, the analytical solution method fails outside of a narrow range of structure function time lags if the ramp amplitude is negative (i.e., the odd-ordered structure function is positive). For data intervals with positive ramp amplitudes, i.e., during unstable thermal conditions, a broader range of structure function time lags is acceptable than for stable stratification data intervals with negative ramps. In earlier surface renewal studies, this mathematical artifact limited the number of stable thermal intervals that were successfully resolved, introducing uncertainty into flux measurements and requiring gap filling strategies (e.g., Shapland et al. 2012c). Van Atta (1977) demonstrated that the sign of the ramp amplitude in a ramp model time series is always opposite of the odd-ordered structure function. If one artificially reverses the sign of the third- and fifth-ordered structure function values, passes them into the Van Atta procedure, the sign of the ramp amplitude is also reversed. To expand the range of acceptable time lags for data intervals with negative ramps, the logger program converts positive third- and fifth-ordered structure function values into negative values, passes the structure function values into the cubic polynomial, and resolves the magnitude of the ramp amplitude using the analytical solution method. Then, the original sign (negative) of the ramp amplitude is reintroduced, according to the sign of the original third-order structure function.

3.4. Latent heat flux density and evapotranspiration

Latent heat flux density is the energy flux density associated with the water vapor mass flux density between the surface and the atmosphere. The latent energy flux density is obtained in the logger program from the energy balance residual.

$$\lambda E = R_n - G - H \tag{13}$$

The tilt-corrected eddy covariance H is used in the energy balance residual equation because it does not require a calibration factor, unlike the surface renewal H. Latent heat flux density is then divided by the latent heat of evaporation (λ) to obtain the mass flux density of water vapor, i.e., ET.

$$ET = \frac{\lambda E}{\lambda} \tag{14}$$

4. SOFTWARE

The program is written in the Campbell Scientific CRBasic language for the CR1000 data logger, but it can be easily modified for most other modern Campbell Scientific loggers. The program is named "RMYS_2HFP_KZ.CR1", an abbreviation for RM Young in Serial mode with 2 Heat Flux Plates and a Kipp and Zonen net radiometer. One can adapt the program for other sensor configurations, but the user should carefully field test the logger program after any modifications. If many new lines of complex code are added to the program, then it may not function properly; especially when the sonic anemometer is sampled in serial rather than analog mode. The program is available for download at sites.google.com/site/ tmshapland.

4.1. Program design

When the program is opened with CRBasic or a text editor, the user first sees the notes describing the title of the program, its contributors, its maintainer, instructions for citing the program, and an overview of the program design and functionality (lines 1-48).

The user next encounters the site-specific user inputs (lines 49-69), including the sonic anemometer and thermocouple heights, the net radiometer calibration constants, the heat flux plate calibration constants, the estimated volumetric water content, and the estimated soil bulk density. A note next to each input describes the parameter and its units. The user should enter the appropriate site-specific values in this section. If the

canopy is no longer actively growing and the distance between the sensor and canopy top is no longer changing, then the user can enter the surface renewal alpha calibration. Parameters that are not site-specific, and therefore should not be changed by the user, are declared in the next section (lines 70-91).

The wiring diagram is described in lines 92-147 using the wire colors of sensors distributed in the United States and in Tab. 1. The instructions indicate where to connect the wires from each sensor to the appropriate logger channels and ports. Note that wire colors could vary for different sensors and by country.

Because CRBasic language is a compiled language, rather than interpreted language, all variables must first be declared at the start of the program. The variable declarations are organized such that the high-frequency variables are first (lines 148-181), the structure function and covariance variables are second (lines 182-205), the variables that are used to calculate the turbulent fluxes using the surface renewal and eddy covariance methods are third (lines 206 – 280), the preliminary *G* and *Rn* are fourth (lines 281-290), and the energy balance and diagnostic variables are last (lines 291-332).

In the next section, the data tables are declared, including the data table for the raw turbulent signals (turb_raw, lines 338-343), the data table for the preliminary fluxes (preflux, lines 348-367), the data table for the preliminary *Rn* and *G* measurements (preRnG, lines 372-381), and the energy balance data table, i.e., the ultimate output of the program (EB, lines 387-412). Next to each term in the EB data table, its meaning is described as a comment. The EB data table terms and their units are also defined in Tab. 2.

4.2. Program execution

The final section of the program, constituting the last third of the lines (425-623), contains the executable commands that instruct the logger on sampling the various instruments and processing the data. The program first samples the high-frequency (10 Hz) turbulent variables, i.e., the three dimensional wind velocities, the sonic temperature, and the thermocouple air temperature. The sonic anemometer is sampled in serial mode (lines 425-439). If the data transfer from the sonic anemometer to the data logger fails during a scan, the character string "NaN" (Not a Number) is recorded, and the logger program is unable to calculate statistics, such as covariance or mean, and hence unable to calculate the energy balance fluxes. To avoid this problem, "NaN" strings are replaced with the values from the previous scan (lines 440-446). The voltage from the reference junction of the thermocouple is sampled and converted to Celsius using the CRBasic thermocouple differential channel function, and the second-, third-, and fifth-order structure function values at a 0.5 time lag are calculated from the sonic temperature and the thermocouple air temperature measurements (lines 447-461). Because the reference temperature used for thermocouple readings in Campbell Scientific data loggers is the panel temperature, which changes slowly, and only the high frequency thermocouple temperature fluctuations are used in surface renewal measurements, environmental shielding of the data logger is not critical, unlike the requirements for making slow-response absolute temperatures measurements. The structure function values are the input statistics for resolving the sonic temperature and air temperature ramp characteristics (Van Atta, 1977) that are used to calculate the surface renewal *H* (Paw U *et al.*, 1995; Spano *et al.*, 1997). The CallTable commands tell the logger to store the high-frequency turbulent signals in the turb_raw data table (line 462) and calculate the structure function values and the wind velocity and sonic temperature covariance statistics in the preflux data table (line 464).

The SlowSequence command is called to decrease the sampling frequency to 1 Hz for the remaining sensors and commands (line 471) that do not require high frequency sampling. Two important system diagnostics, the battery voltage and logger temperature, are sampled on lines 473 and 474. The voltage signal from the net radiometer and the two heat flux plates are sampled using the VoltDiff command (lines 475-477), and the soil thermocouple is sampled on line 478.

The commands for processing the raw turbulence data into corrected fluxes are also written within the SlowSequence structure. Due to the particulars of the SlowSequence command, the preliminary turbulent statistics, i.e., the wind velocity and sonic temperature covariance statistics and the structure function values, must be calculated before the other post-processing functions are executed. As a result, the preliminary turbulent statistics in the preflux data table, and hence the final eddy covariance and surface renewal fluxes from the logger program and the diagnostic variables associated with the velocity field, are based on the first 1799 seconds of data in the 30 minute (1800 second) interval.

The wind velocity, sonic temperature covariance statistics, and the structure function values are called into the program from the preflux table (line 488). The covariance statistics are used to calculate the two-dimensional coordinate rotation angles (lines 492-495). The rotation is applied to the vertical velocity and sonic temperature covariance to obtain the tilt-corrected vertical temperature flux (line 496), which is converted to *H* (line 497). The coordinate rotation is also applied to the wind velocity covariance statistics to obtain the

Variable	Definition	Units
Tpanel	Logger temperature	C
BattVolt	Mean battery voltage	V
Tc0	Mean air temperature measured by the thermocouple	C
St1	Mean soil temperature	C
u_bar	Mean horizontal wind speed	m s^{-1}
ustar	Friction velocity	m s^{-1}
tke	Turbulent kinetic energy normalized by mass	m^{-2} s^{-2}
tau	Momentum flux density	N m^{-2}
pitch	Sonic anemometer pitch angle	Degrees
azimuth	Wind direction angle	Degrees
Tsa	Sonic temperature ramp amplitude	K
TsDS	Sonic temperature ramp period	s
Tca	Air temperature ramp amplitude measured by thermocouple	C
TcDS	Air temperature ramp period measured by thermocouple	s
Rn	Net radiation	W m^{-2}
G	Ground heat flux density	W m^{-2}
TcH_SR	Surface renewal sensible heat flux density measured by the thermocouple	W m^{-2}
TsH_SR	Surface renewal sensible heat flux density measured by the sonic temperature	W m^{-2}
H_ECraw	Eddy covariance sensible heat flux density without tilt correction	W m^{-2}
H_ECrot	Eddy covariance sensible heat flux density with tilt correction	W m^{-2}
LE_ECraw	Latent heat flux density as the energy balance residual using *Rn*, *G*, and *H_ECraw*	W m^{-2}
LE_ECrot	Latent heat flux density as the energy balance residual using *Rn*, *G*, and *H_ECrot*	W m^{-2}

Tab. 2 - Definition of variables in the final output table (i.e., data table EB) of the logger program.
Tab. 2 - Definizioni delle variabili nella tabella dei risultati (cioe' la data table EB) del programma per datalogger.

tilt-corrected momentum flux density (line 499). The mean horizontal wind speed, the turbulent kinetic energy, the wind pitch angle, and the wind azimuth angle are calculated (lines 500-510) for use as diagnostic variables in data quality control by the user.

Starting on line 516, the ramp amplitude and ramp period from the sonic temperature are resolved using the Van Atta (1977) procedure. The sign of any positive third- and fifth-order structure function values are changed to negative values to ensure that the analytical solution succeeds over a greater range of lags (line 517 and 518). The cubic polynomial coefficients, p (Equation 11b) and q (Equation 11c), are calculated from the structure function values (lines 519 and 520). Another term, D, is derived from p and q to determine whether the cubic polynomial has three real roots or only one real root (line 521). If D is less than or equal to zero, the cubic polynomial is solved trigonometrically (lines 522-533). If D is greater than zero, the cubic polynomial is solved algebraically (lines 534-544). After the computation, the sign of the ramp amplitude in the sonic temperature data is recovered, i.e., set to the opposite sign as the original third-order structure function, and the ramp period is calculated (line 547-553). The ramp characteristics are used to calculate the surface renewal H (line 555). The surface renewal H from the thermocouple is calculated in the same manner on lines 557-597.

The net radiometer voltage signal is converted into *Rn* using its calibration factor (line 600). The net radiometer voltage signal, *Rn*, the ground heat flux plate voltage signals, and the soil thermocouple temperature are stored in the preRnG data table (line 603). Unlike the Kipp and Zonen NR-Lite instrument, some net radiometers require a correction that is dependent on wind speed. Although the preRnG data table could have been called earlier in this particular program, it is called after the horizontal wind speed calculation to facilitate modifying the program for other net radiometers.

The change in soil temperature from the beginning to the end of the measurement interval is calculated on line (607), and it is used to calculate the energy stored in the soil layer above the ground heat flux plates (line 610). The heat flux plate voltage signal is converted to an energy flux density using the plate calibration

coefficients (line 613 and 614). The mean of the two ground heat flux plates is added to the energy storage in the soil layer above the plates to obtain *G* (line 615).
After *Rn*, *H*, and *G* are determined, λE is calculated as the residual of the energy balance (line 619). The energy balance terms and the diagnostic variables are output on the EB data table (line 621).

5. RESULTS AND DISCUSSION

5.1. Comparison of energy balance terms from the logger program, EdiRe, and R

The output of the logger program is compared to the output of other flux processing programs to ensure that it is functioning properly. EdiRe does not have functions for *G* and *Rn* calculations, so comparing EdiRe and the logger program for these terms was not possible. These functions were written in the R computer language, and there were no differences in the *Rn* and *G* terms calculated in R and the logger program (Fig. 1a - b).
The logger-calculated *H* was compared against EdiRe and R (Fig. 1c). There were no differences between the tilt-corrected eddy covariance *H* from the logger program and from the R program. The R program was modified to calculate *H* (and the other turbulent statistics) on same 1799 second interval as the logger program. The differences in the *H* calculations between the logger program and EdiRe that arose from the additional second of data in the averaging interval are imperceptible in the regression analysis plots (Fig. 1c) and rounded statistics (Tab. 3). While it is technically correct to include the entire 1800 second interval in the turbulent flux calculations, because the *Rn* and *G* terms are calculated on this interval, it is clear that the final second of data does not appreciably impact the results. The error stemming from such minor discrepancies in the data interval is readily outweighed by the other errors associated with measuring turbulent fluxes (e.g., Foken 2008), including errors associated with uncertainty in the appropriate data interval for capturing the largest turbulent eddy scales (Lee *et al.*, 2004).
The latent heat flux density was calculated as the residual of the energy balance. There were no differences between λE flux calculations by the logger

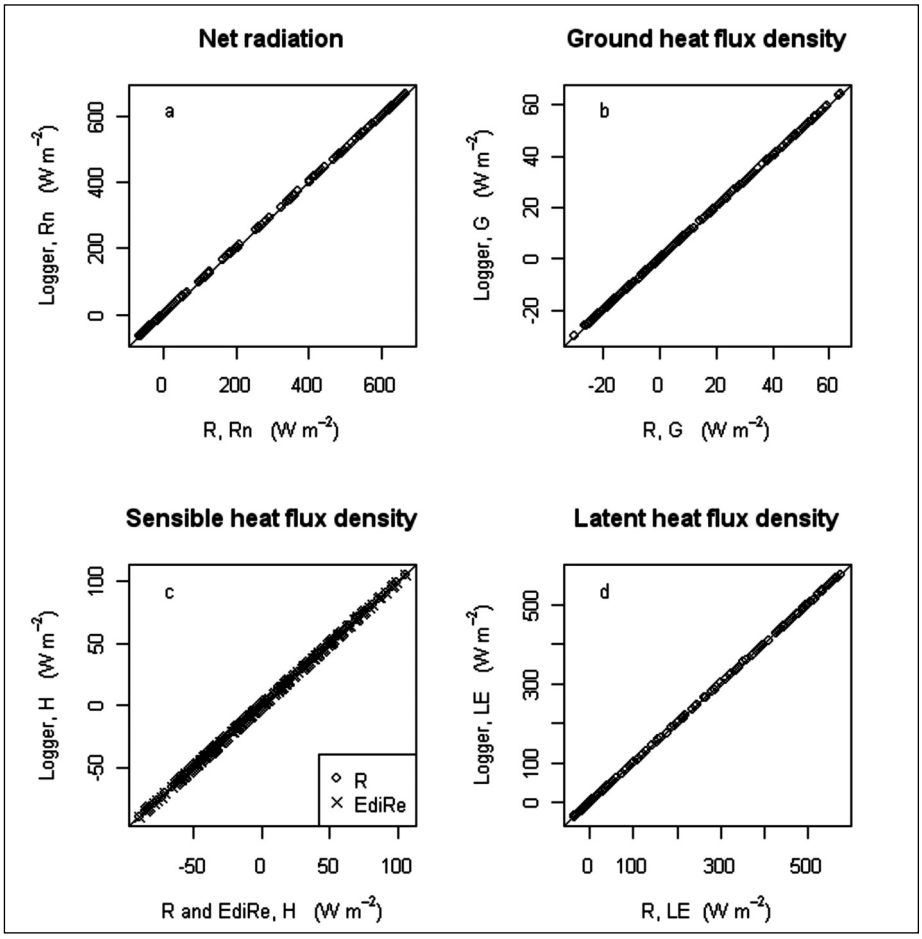

Fig. 1 - Linear regression plots for energy balance terms calculated by the logger program against energy balance terms calculated in R and EdiRe, including (a) net radiation, (b) ground heat flux density, (c) sensible heat flux density, and (d) latent heat flux density.
Fig. 1 - Regressioni lineari fra i componenti del bilancio energetico calcolati dal programma per datalogger e quelli calcolati con EdiRe e R: radiazione netta (a), flusso di calore nel suolo (b), flusso di calore sensibile (c) e flusso di calore latente (d).

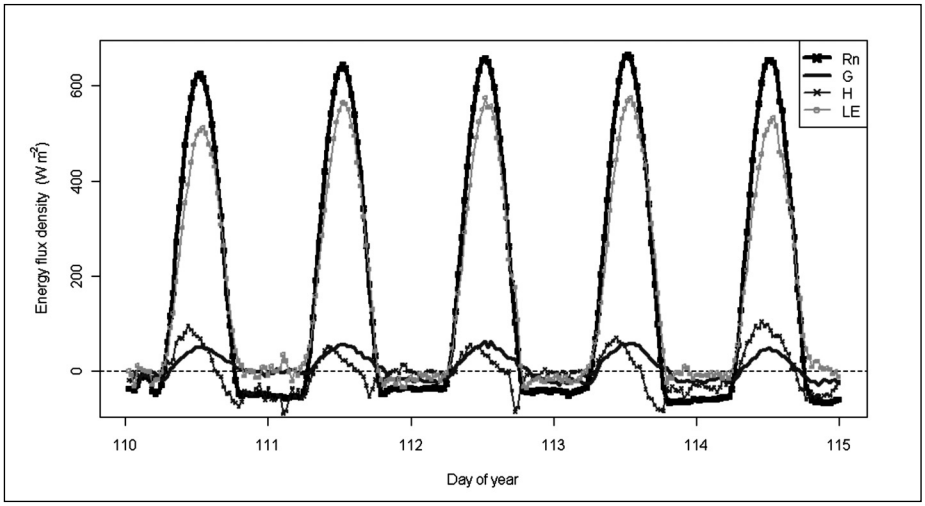

Fig. 2 - Diurnal energy balance flux densities.
Fig. 2 - Flussi giornalieri del bilancio energetico.

program and R (Fig. 1d). To make the comparison in the λE calculation between EdiRe and the logger program, the *Rn* and *G* terms were taken from the logger and *H* was taken from EdiRe because *Rn* and *G* were not calculated in EdiRe. The differences in λE between the logger program and EdiRe, arising from the differences in the data interval used in the *H* calculation, are negligible.

5.2. Interpretation of diurnal energy balance terms

Unlike laboratory experiments, ecosystem scale flux measurements are difficult to validate because experimental conditions cannot be controlled. An examination of the individual energy balance terms during fair weather conditions, such as those encountered in the present study, can provide some confirmation that the flux tower measurements and post-processing calculations are reasonable. The net radiation is positive during the day as the surface receives more radiation than it loses (Fig. 2), and negative at night as the surface loses more radiation than it receives, exhibiting the diurnal curve expected for sunny springtime days in a Mediterranean climate. The ground heat flux density also follows the expected diurnal curve (Fig. 2), and its greatest positive value is about 10% of the maximum *Rn*, which is reasonable for closed canopies (Allen *et al.*, 1998). It is positive during the daytime because energy is conducted from the surface into the ground, and negative at night as more energy is lost from the surface than received. The diurnal pattern in *G* is generally smooth, although there are small deviations likely resulting from sunflecks impinging on the ground directly over the ground heat flux plates. The ground heat flux density is measured at discrete spatial points, whereas the turbulent fluxes are indicative of broader areas, so errors stemming from the incongruity in the footprint of the turbulent fluxes and the available energy terms are expected in the energy balance measurements (Foken, 2008).

During the mornings, *H* was positive (Fig. 2), but in the afternoon it was negative. This is typical of actively transpiring crops in arid climates, where the crop canopy tends to be cooler than warmer air that moves over the surface in the afternoon due to regional advection. The additional sensible heat from regional advection contributes to water vaporization, so afternoon λE values were sometimes greater than the *Rn* values. During the evenings of day 110, 113, and 114, there was sufficient turbulent energy to drive

	R		EdiRe	
	m =	R^2 =	m =	R^2 =
Net radiation	1.00	1.00	--	--
Ground head flux density	1.00	1.00	--	--
Sensible heat flux density	1.00	1.00	1.00	1.00
Latent heat flux density	1.00	1.00	1.00	1.00

Tab. 3 - Linear regression coefficients through the origin for energy balance terms calculated by the logger program against energy balance terms calculated in R and EdiRe.
Tab. 3 - Coefficienti delle regressioni lineari forzate attraverso l'origine fra le componenti del bilancio energetico, calcolate dal programma datalogger e quelle calcolate con EdiRe e R.

negative sensible heat transfer. On the other hand, the evenings of day 111 and 112 showed *H* values near zero, suggesting that the eddy covariance technique could not resolve the flux or that little turbulent transfer was taking place.

The latent energy flux density follows the expected diurnal curve over a crop with adequate water during fair weather (Fig. 2). Net radiation is the dominant energy source for *ET*, so the λE values tracks the changes in *Rn* during the daytime. Over an actively transpiring crop, it is expected that the majority of the available energy during positive *Rn* conditions is partitioned into λE rather than *H* and *G*. During windy nights (i.e., days 110, 113, and 114), λE was near zero, whereas it was negative during calm nights, indicating condensation. While some condensation may have been occurring, there may also have been a slight bias in the estimation of the available energy terms (*Rn* and *G*), and therefore the negative λE values would be artifacts of the energy balance residual method. Nevertheless, the daytime contribution to λE greatly outweighs the nighttime contribution, so uncertainties in nighttime values are interesting but relatively unimportant.

5.3. Comparison of surface renewal and eddy covariance calculations of sensible heat flux density

The high coefficients of determination in the alpha calibration regressions for the surface renewal *H* measured with the sonic temperature and thermocouple and the sonic temperature (Fig. 3a and

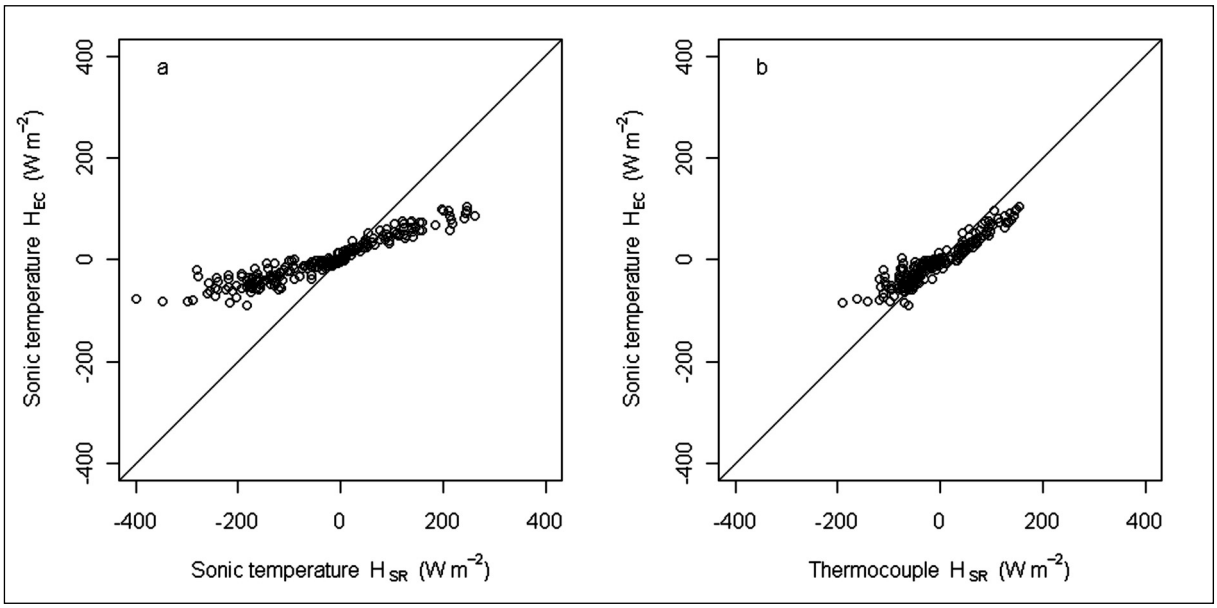

Fig. 3 - Plots of eddy covariance sensible heat flux density (H_{EC}) against surface renewal sensible heat flux density (H_{SR}) using the sonic and thermocouple temperatures. In (a) the sonic temperature is used for both the surface renewal and eddy covariance calculations, whereas in (b) the thermocouple temperature is used for the surface renewal calculation.

Fig. 3 - Regressioni fra il flusso di calore sensibile misurato con Eddy Covariance (EC) e quello misurato con Surface Renewal (SR) usando le temperature dell'anemometro sonico e delle termocoppie. In (a) la temperatura misurata dall'anemometro sonico è usata sia per i calcoli di EC che per i calcoli di SR. In (b) la temperatura delle termocoppie è usata per SR.

	Unstable		Stable		All	
	m =	R^2 =	m =	R^2 =	m =	R^2 =
Sonic temperature	0.42	0.93	0.24	0.88	0.29	0.84
Thermocouple	0.62	0.94	0.57	0.85	0.60	0.89

Tab. 4. - Linear regression coefficients through the origin for surface renewal sensible heat flux density against eddy covariance sensible heat flux density using either the sonic temperature or the thermocouple for the surface renewal calculation.

Tab. 4 - Coefficienti delle regressioni lineari forzate attraverso l'origine fra il flusso di calore sensibile calcolato con Eddy Covariance e calcolato con Surface Renewal, usando o la temperatura misurata dall'anemometro sonico o la temperatura misurata dalle termocoppie, per il calcolo con Surface Renewal.

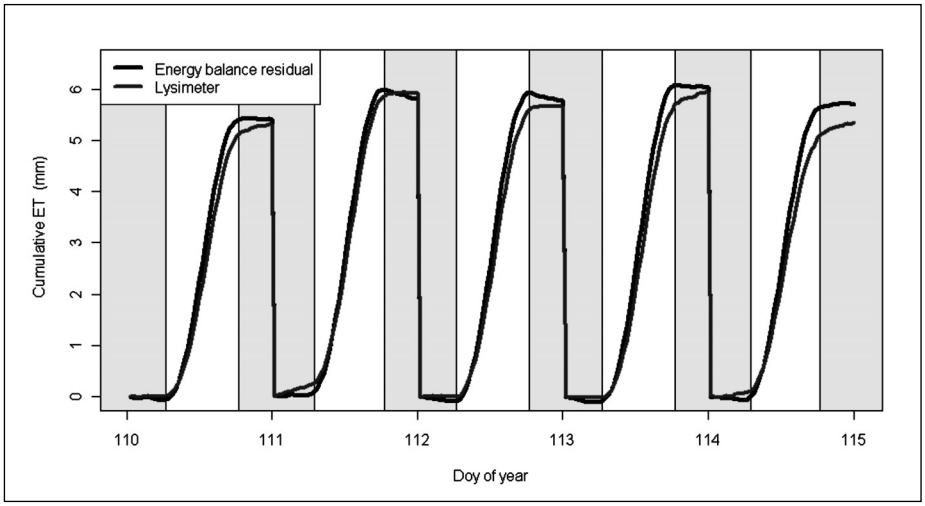

Fig. 4 - Cumulative daily evapotranspiration measured from the flux tower and from the lysimeter. Shaded background areas indicate negative net radiation values.
Fig. 4 - Evapotraspirazione cumulata giornaliera, acquisita mediante la torre di misura dei flussi e dal lisimetro. Aree a sfondo grigio indicano valori negativi di radiazione netta.

b, Tab. 4) are typical of the alpha calibration regressions from other studies (Paw U *et al.*, 1995; Snyder *et al.*, 1996; Spano *et al.*, 1997; Paw U *et al.*, 2005; Shapland *et al.*, 2012a), demonstrating that the logger program results are reasonable. The alpha calibration is lower when the sonic temperature is used for the scalar in the surface renewal calculation rather than the thermocouple signal for both unstable and stable conditions (Fig. 3a and b; Tab. 4). This occurs because the thermal inertia of the thermocouple attenuates the high frequency components of the time domain signal to a greater extent than the sampling volume spatial averaging of the sonic anemometer, leading to an underestimation of the scalar ramp characteristics (Shapland *et al.*, 2012b). As a result of this data artifact, the surface renewal *H* from the thermocouple signal aligns better with the eddy covariance *H* compared to the surface renewal *H* from the sonic temperature. Work is currently in preparation for the evaluation of a method for compensating the thermocouple signal for surface renewal measurements, and future versions of the logger program will include online thermocouple compensation (Shapland *et al.*, 2012b).

5.4. Comparison of cumulative daily evapotranspiration from the logger program and the lysimeter

The daily cumulative *ET* values from the logger program and the lysimeter agree well (Fig. 4). On most days, the cumulative *ET* from the logger program was slightly higher than the values from the lysimeter; however, the tower measurements represent fluxes from a broader and different area than the lysimeter measurements. Given that the wheat stand in the lysimeter was about 10 cm shorter and less dense than the plants in remainder of the field, higher *ET* values from the flux tower were expected. There are numerous other potential sources of error in *ET* measurements from flux towers (Lee *et al.*, 2000) and lysimeters (Pruitt and Angus, 1960), so the disparity between the measurement systems is not unreasonable.

6. CONCLUSIONS

The turnkey logger program was tested against independent software programs to demonstrate that the energy balance fluxes are correctly calculated. The diurnal energy balance curves from the flux tower and logger program follow the expected patterns for a crop field with adequate water in fair weather conditions, and the *ET* measurements from the flux tower agree well with the lysimeter measurements. The logger program renders micrometeorological methods more accessible for agricultural researchers and facilitates data processing and management. The output table containing the energy balance terms and the diagnostics variables can be downloaded using a remote or direct connection, adding significant convenience for program users during site visits.
The software presented here represents a core program that users can easily modify for other sensor configurations. The program and supplementary material can be downloaded at sites.google.com/site/tmshapland. We anticipate future releases of updated versions of the program as this is an ongoing project in our research efforts.

7. ACKNOWLEDGEMENTS

Partial support for this research was provided by J. Lohr Vineyards & Wines, the National Grape and Wine Institute, a NIFA Specialty Crops Research Initiative grant to AJM, and USDA-ARS CRIS funding (Research Project #5306-21220-004-00). The authors

thank Diganta Adhikari, Frank Anderson, Cayle Little, Honza Rejmanek, Alfonso Russo, Mike Mata, and Gwen Tindula for their contributions and assistance in field testing the program.

8. REFERENCES

Allen R.G., Pereira L.S., Raes D., Smith M., 1998. Crop evapotranspiration: Guidelines for computing crop water requirements. FAO Irrigation and Drainage Paper 56. FAO, Rome, Italy.

DeVries D.A., 1963. Thermal properties of soils. *In:* Van Wijk, W.R. (ed.) Physics of the plant environment. North-Holland Publishing Co., New York, NY., U.S.A., 382 pp.

Doorenbos J., Pruitt W. O., 1977. Crop water requirements. FAO Irrigation and Drainage Paper 24. FAO, Rome, Italy.

DWR (Department of Water Resources), 2005. California Water Plan Update, Bulletin 160-05. California Department of Water Resources, Sacramento, CA., U.S.A.

Foken T., 2008. The energy balance closure problem. Ecological Applications, 18(6):1351-1367.

Jensen M.E., Burman R.D., Allen R.G., 1990. Evapotranspiration and irrigation water requirements. ASCE Manuals and Reports on Engineering Practice 70, American Society of Civil Engineers, New York, NY, U.S.A., 332 pp.

Mauder M., Foken T., Clement R., Elbers J. A., Eugster W., Grunwald T., Heusinkveld B., O. Kolle, 2008. Quality control of CarboEurope flux data – Part 2:Inter-comparison of eddy-covariance software. Biogeosciences, 5:451-462.

Lee X., Massman W.J., Law B.E., (eds.) 2004. Handbook of micrometeorology: A guide for surface flux measurement and analysis. Kluwer Academic Publishers, London, U.K., 250 pp.

Moratiel R., Martínez-Cob, A., 2011. Evapotranspiration of table grape trained to a gable trellis system under netting and black plastic mulching. Irrigation Science, 30(3):167-178.

Paw U K.T., Qiu J., Su H.B., Watanabe T., Brunet Y., 1995. Surface renewal analysis: a new method to obtain scalar fluxes without velocity data. Agricultural and Forest Meteorology, 74:119-137.

Paw U K.T., Snyder R.L., Spano D., Su H.B., 2005. Surface renewal estimates of scalar exchange. *In:*Hatfield, J.L. (ed.) Micrometeorology of agricultural systems. Agronomy Society of America, Madison, WI, U.S.A., 584 pp.

Pruitt W.O., Angus D.E., 1960. Large weighing lysimeter for measuring evapotranspiration. Transactions of the American Society of AgriculturalEngineers, 3(18):13-15.

R Development Core Team, 2012. R: A language and environment for statistical computing. R Foundation for Statistical Computing, Vienna, Austria.

Shapland T.M., McElrone A.J., Snyder R.L., Paw U, K.T., 2012a. Structure function analysis of two-scale scalar ramps. Part II: ramp characteristics and surface renewal flux estimation. Boundary-Layer Meteorology. 145:27-44.

Shapland T.M., Snyder R.L., Paw U K.T., and McElrone A.J., 2012b. Thermocouple frequency response compensation for surface renewal sensible heat flux measurements. (*In preparation*)

Shapland T.M., Snyder R.L., Smart D.R., Williams L.E., 2012c. Estimation of actual evapotranspiration in winegrape vineyards located on hillside terrain using surface renewal analysis. Irrig. Sci. 30(6): 471-484.

Snyder R.L., Spano D., Paw U K.T., 1996. Surface renewal analysis of sensible and latent heat flux density. Boundary-Layer Meteorology, 77:249-266.

Spano, D., Snyder, R.L., Duce, P., Paw U, K.T., 1997. Surface renewal analysis for sensible heat flux density using structure functions. Agricultural and Forest Meteorology, 86:259-271.

Synder R., Orang M., Geng S., Matyac S., Sarreshteh S., 2005. SIMETAW (Simulation of Evapotranspiration of Applied Water). California Water Plan Update 2005,Vol. 4: Reference guide, California Department of Water Resources, Sacramento, CA, U.S.A. Tanner, C.B., Thurtell, G.W., 1969. Anemoclinometer measurements of Reynolds stress and heat transport in the atmospheric surface layer. Research and Development Technical Report ECOM 66-G22-F to the US Army Electronic Command, Department of Soil Science, University of Wisconsin, Madison, WI, U.S.A.

Swinbank W.C., 1951. The measurement of vertical transfer of heat and water vapor by eddies in the lower atmosphere. Journal of Meteorology, 8(3):135-145.

Van Atta C.W., 1977. Effect of coherent structures on structure functions of temperature in the atmospheric boundary layer. Archives of Mechanics, 29:161-171.